analytical chemistry

Letter

pubs.acs.org/ac

Approaching Sensitivity of Tens of Ions Using Atomically Precise Cluster−Nanofiber Composites

Atanu Ghosh,[†] Vedhakkani Jeseentharani,[†] Mohd Azhardin Ganayee,[†] Rani Gopalakrishnan Hemalatha,[†] Kamalesh Chaudhari,[†] Cherianath Vijayan,[‡] and Thalappil Pradeep*[,†]

[†]DST Unit of Nanoscience (DST UNS) and Thematic Unit of Excellence (TUE), Department of Chemistry, Indian Institute of Technology Madras, Chennai 600 036, India

[‡]Department of Physics, Indian Institute of Technology Madras, Chennai 600 036, India

Supporting Information

ABSTRACT: A new methodology has been demonstrated for ultratrace detection of Hg^{2+}, working at the limit of a few tens of metal ions. Bright, red luminescent atomically precise gold clusters, Au@BSA (BSA, bovine serum albumin), coated on Nylon-6 nanofibers were used for these measurements. A green emitting fluorophore, FITC (fluorescein isothiocyanate), whose luminescence is insensitive to Hg^{2+} was precoated on the fiber. Exposure to mercury quenched the red emission completely, and the green emission of the fiber appeared which was observed under dark field fluorescence microscopy. For the sensing experiment at the limit of sensitivity, we have used individual nanofibers. Quenching due to Hg^{2+} ions was fast and uniform. Adaptation of such sensors to pH paper-like test-strips would make affordable water quality sensors at ultralow concentrations a reality.

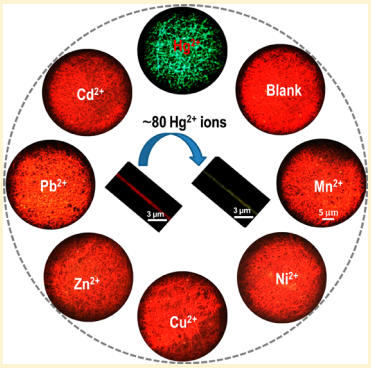

Noble metal nanoparticles (NM NPs) and their atomically precise analogs called quantum clusters (QCs) (also known as monolayer protected clusters, nanomolecules, and quantum dots) are new paradigms in the ultralow detection of various species due to their unique electronic structure and versatile surface functionalization.[1−13] While limits of sensitivity have reached zeptomole levels[14] with such systems, adaptation of these materials into useful devices has not been advancing significantly. A combination of ultralow sensitivity with affordability and adaptability to devices in the field would make cluster-based sensors available as consumer products. One of the major expanding nanoscale platforms for these applications is electrospun nanofibers[15−22] which enables extremely small quantities of materials distributed over large areas with high uniformity. This platform also enables measurements using optical techniques (in the visible window) at single fiber level, as they are of submicrometer dimensions, larger than the diffraction limit of visible light.

Atomically precise clusters of noble metals, due to their discrete energy states, show inherent luminescence.[23] In a few such clusters, emission occurs in the visible region of the electromagnetic spectrum, observable even to the naked eye.[24,25] Cluster luminescence has been shown to be sensitive to many environmental factors such as chemical contamination, pH, temperature, etc.[23,26] Molecular luminescence of the clusters is enhanced upon trapping the clusters in cavities as well as confining them in containers.[27,28] The nonradiative relaxation channels are blocked by such methods resulting in enhanced emission.[27,29]

Such clusters confined to micrometer (μm) dimensions can be useful in optical microscopy-based detection. An application toward this was demonstrated recently using mesoflowers in which zeptomole detection of the explosive trinitrotoluene (TNT) was accomplished.[14] Confining clusters on nanofibers is a more versatile strategy in the optical microscopy context as it enables easy attachment on other substrates besides allowing direct observation. In this communication, we demonstrate single fiber-based detection of mercuric ion nearly at the limit of single ion concentration. Adaptation of such sensors to pH paper-like test-strips would make affordable water quality sensors at ultralow concentrations a reality.

Electrospinning has become a simple and versatile technique for the preparation of nanofibers which possesses many advantages including controlled morphology and large surface area-to-volume ratio.[30] They have found applications in tissue engineering, filtration, electronic devices, catalyst supports, and sensing devices.[31] Electrospun nanofibers could act as suitable substrates to load clusters.

Mercury in both organic and inorganic forms is one of the most hazardous environmental contaminants. Different approaches have been used for the determination of trace levels of mercury.[32−36] Fluorescence-based techniques have great importance in the determination of ionic mercury.[9,14] However, as we understand the implications of even trace levels of heavy

Received: July 25, 2014
Accepted: October 22, 2014
Published: October 22, 2014

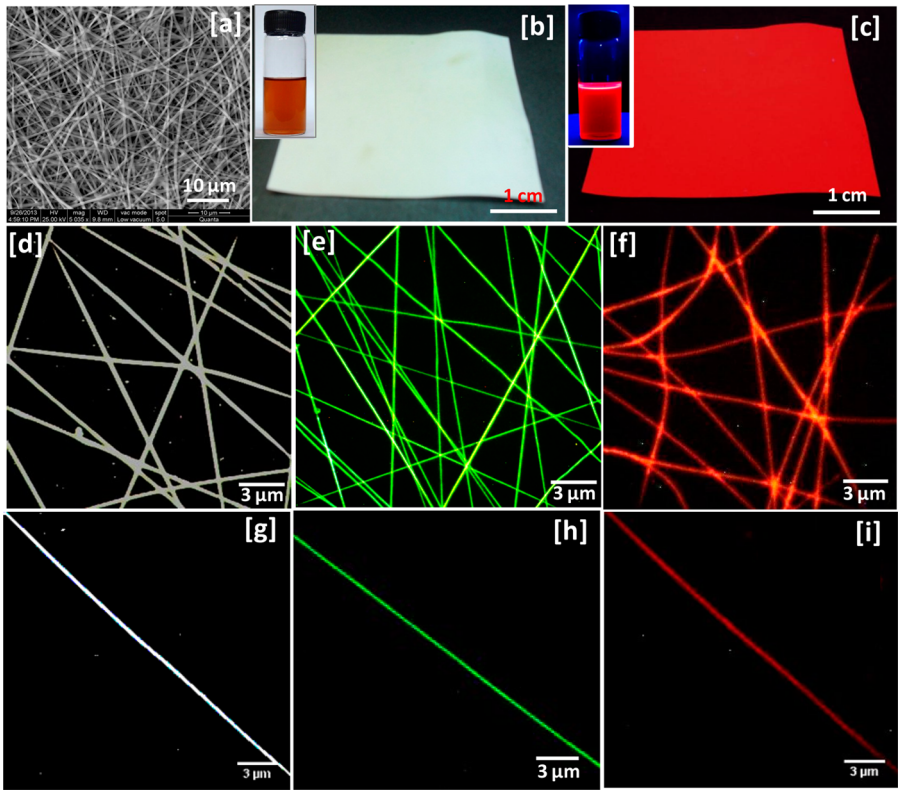

Figure 1. (a) SEM image of a fiber mat. (b) Visible light photograph of the Au@BSA/N6 fiber mat (inset: Au@BSA cluster solution under visible light). (c) Photograph of the same mat under UV light (inset: Au@BSA cluster solution under UV light). (d) Optical image of a few Au@BSA/FITC/N6 fibers prepared on a glass slide. (e) Fluorescence image of FITC/N6 fibers. Green emission is due to FITC. (f) Fluorescence image of Au@BSA/FITC/N6 fiber. As red luminescence dominates over green, the fibers showed only red color. (g), (h), and (i) are the corresponding images of a single fiber.

metals, methods for ultrasensitive, field-implementable solutions have to be developed, working at the limit of single ions.

The appproach used in the present experiment is as follows. The red luminescence of atomically precise gold clusters is quenched by Hg^{2+} ions in water. The quenching is even more prominent on nanofibers as the cluster emission is enhanced on them as nonradiative relaxation channels are reduced. As the disappearnce of cluster luminescence (due to Hg^{2+} exposure) will lead to a nonluminescent or black fiber mat, a fluorophore, whose luminescence is insensitive to Hg^{2+}, is precoated on the fiber. The fluorophore used here is fluorescein isothiocyanate (FITC) which emits in green. As a result, when the luminescence of gold clusters disappear, that of FITC becomes visible. Although the fiber has emissive clusters and has FITC anchored on it initially, due to the dominance of the fluorescence of the former, the fiber appears red initially in the luminesence image. Exposure to mercury quenches the red emission completely, and the green emission of the fiber mat appears. In the in-between concentrations, intermediate colors are seen. The detection can happen down to a single fiber level with a simple fluorescence microscope, which requires just a few Hg^{2+} ions for observable color change, enhancing detection limits.

EXPERIMENTAL SECTION

Chemicals. Nylon-6 (N6, Molecular weight 10 031 g/mol), fluorescein isothiocyanate (FITC), and bovine serum albumin (BSA) were purchased from Sigma-Aldrich. Formic acid and divalent acetates of mercury, zinc, copper, nickel, manganese, lead, and cadmium were purchased from Merck. Deionized water was used for all experiments. All chemicals were used directly without any additional purification.

Synthesis of Au@BSA Cluster. The Au@BSA nanoclusters with red luminescence were prepared following a reported method[37] by adding 10 mL of aqueous solution of $HAuCl_4$ (6 mM) to 10 mL of BSA (25 mg/mL in water) under vigorous stirring for 5 min. The pH of the solution was adjusted around 11.0 with the addition of NaOH (1 mL, 1 M). The reactions were kept for 24 h. The solution turned from pale yellow to dark orange, with deep red emission, indicating the formation of Au@BSA nanoclusters. The sample was stored at 4 °C.

Synthesis of N6 Fiber Mat. N6 fiber mat was prepared by slight modification of an earlier report.[30] 4.5 g of N6 polymer was dissolved in 10 mL of formic acid, and the mixture was stirred at 60 °C for 15 h to obtain a transparent homogeneous solution. The prepared N6 solution was loaded into a 2 mL plastic syringe equipped with a needle of 0.8 mm outer diameter and 0.6 mm inner diameter. A high voltage was applied between the needle and the collector. The syringe was fixed on an electric syringe pump set to maintain a constant flow rate of 0.1 mL/h. Positive potential was applied to the needle by a high-voltage power supply. The voltage used for electrospinning was 28 kV. The distance between the needle tip and the collector was 16 cm. Nanofibers were collected on an aluminum sheet mounted on a cylindrical drum collector, which rotated at a speed of 2500 rpm. The electrospun fiber mat was prepared by spinning the respective solutions for 1 h on aluminum sheets.

dx.doi.org/10.1021/ac502779r | Anal. Chem. 2014, 86, 10996−11001

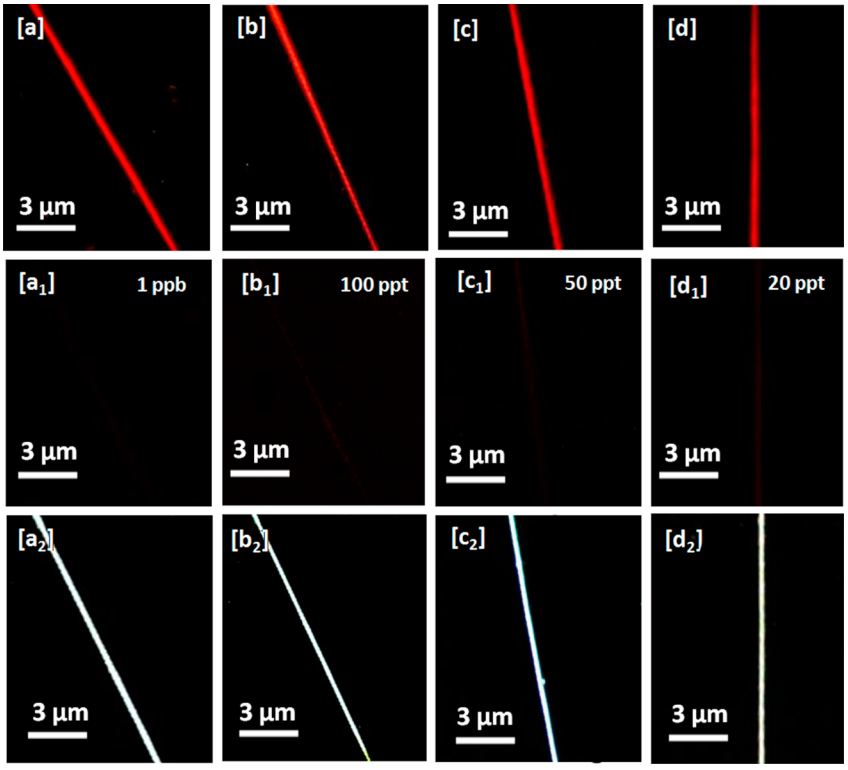

Figure 2. Images for the sensing experiment which was done using the Au@BSA/N6 single fiber. Fluorescence images (a, b, c, and d) of single fibers before the addition of Hg^{2+} ion solution. (a_1, b_1, c_1, and d_1) Flourescence images of the respective fibers (a, b, c, and d) after the addition of 1 ppb and 100, 50, and 20 ppt of Hg^{2+} ion solutions, respectively. The red color was quenched completely in 1 ppb, but in the case of 20 ppt, a faint red color can be seen upon closer examination. Optical images of the corresponding fibers are shown in a_2, b_2, c_2, and d_2, respectively. It shows that fiber morphology is intact after the addition of the Hg^{2+} ion solution and only luminescence of the fiber was quenched.

Synthesis of Au@BSA/N6 Fiber Mat. The above prepared fiber mat was dipped in an as-synthesized aqueous Au@BSA cluster solution for 10 min. Then, it was washed three times with water to remove the excess loosely bound clusters. After water washing, the clusters were present only on the fibers. It is shown in the case of the single fiber experiment (Figures 2 and 4i).

Synthesis of Au@BSA/FITC/N6 Multiple and Single Fiber. 4.5 g of N6 polymer and 3 mg of FITC were dissolved in 10 mL of formic acid, and the mixture was stirred at 60 °C for 15 h to obtain a transparent homogeneous solution. Electrospining of the solution was done in the same way. The FITC/N6 fibers were collected on a glass slide instead of an aluminum sheet. To examine the FITC/N6 single fibers, they were collected on the glass slide only for 2−3 s. The fibers show green luminescence under a microscope due to FITC. The Au@BSA cluster solution was added to the FITC/N6 fibers on the glass side drop by drop and dried in air. Then, the slide was carefuly washed 2−3 times with water to remove the excess cluster present on the slide and dried in air to get red luminescent Au@BSA/FITC/N6 fibers.

Sensing Experiment. For the single fiber sensing experiment, we have placed the glass slide containing the fiber under the microscope. About 2.5 μL of Hg^{2+} ion solution was added on the fiber. A fluorescence image of the seleted fiber was taken before and after the addition of Hg^{2+}.

UV−vis spectra were recorded using a PerkinElmer Lambda 25 spectrophotometer. Scanning electron microscopic (SEM) images and energy-dispersive analysis of X-ray (EDAX) studies were performed using a FEI QUANTA-200 SEM. The photoexcitation and luminescence (PL) studies were done using a NanoLog HORIBA JOBINYVON spectrofluorimeter. Luminescence spectra of fiber mats were collected using 488 nm LASER excitation in a RAMAN spectrometer. X-ray photoelectron spectroscopy (XPS) measurements were conducted using an Omicron ESCA Probe spectrometer with unmonochromatized Al Kα X-rays (energy = 1486.6 eV). Fluorescence imaging measurements were done with the Cytoviva HSI system containing an Olympus BX-41 microscope equipped with a Dage high resolution camera and a Specim V10E spectrometer. Dark field fluorescence microscopy was used with an excitation band at 492 ± 18 nm, and emission was collected using a triple pass emission filter DAPI/FITC/TEXAS RED (DAPI, 452−472 nm; FITC, 515−545 nm; TEXAS RED, 600−652 nm). Further details of the experiment are presented in the Supporting Information.

RESULTS AND DISCUSSION

The materials used in this study, namely, red luminescent gold clusters protected by BSA (Au@BSA; BSA, bovine serum albumin), were synthesized by a reported procedure, and details are presented in the Experimental Section.[37] In view of the properties already known of this material, we list only the essential details here. The Au@BSA cluster contains a core of 25 atoms of Au protected with the protein, and BSA shows an optical absorption feature at 520 nm.[37] The photoluminescence spectrum (Figure S1, Supporting Information) shows an emission maximum at 670 nm when excited at 365 nm, at room temperature.

dx.doi.org/10.1021/ac502779r | Anal. Chem. 2014, 86, 10996−11001

A sensor platform was developed using electrospun nanofibers prepared by N6. Preparation of the fibers was discussed in detail in the Experimental Section. The SEM images of the N6 fiber mat showed high uniformity (Figure 1a). The fiber diameters range from 180 to 260 nm (distribution has been given in Figure S2, Supporting Information). The N6 fiber mat was dipped in an as-synthesized Au@BSA cluster solution for 10 min for adsorption of the clusters on the fibers, and the mat was washed with water three times to remove the excess cluster solution. The sample was labeled as a Au@BSA/N6 fiber mat. The mat appears white in visible light (Figure 1b) and red in UV light (Figure 1c). The solution of Au@BSA in visible light and UV light is shown in the insets of Figure 1b,c, respectively.

In order to observe individual fibers, electrospinning was performed on glass slides for short periods. FITC incorporated N6 nanofiber, labeled as FITC/N6, was produced by the electrospinning of a solution which contains N6 and FITC. The FITC/N6 fibers on the glass slides were coated with the Au@BSA cluster and washed 2−3 times carefully to remove the excess cluster present on the slides. The cluster coated fibers are labeled as Au@BSA/FITC/N6. Details of the preparation of FITC/N6 and Au@BSA/FITC/N6 fibers are given in the Experimental Section. The optical image of a collection of Au@BSA/FITC/N6 fibers is shown in Figure 1d. Fluorescence images of FITC/N6 and Au@BSA/FITC/N6 fibers are shown in Figure 1e,f, respectively. FITC/N6 fibers showed a green color due to the green luminescence of FITC (Figure 1e). As red luminescence dominates over green, the Au@BSA/FITC/N6 fibers showed only red color (Figure 1f). The same images for single fibers are shown in Figure 1g−i. For the sensing experiment at the limit of sensitivity, we have used these individual fibers.

The concentration dependence (mercuric ion) of luminescence quenching of individual Au@BSA/N6 fibers is shown in Figure 2. The quenching due to Hg^{2+} ions was performed with various concentrations ranging from 1 ppb to 20 ppt. These experiments were performed by dropping 2.5 μL of the appropriate quantity of aqueous Hg^{2+} solution on the fiber and measuring the fluorescence image. Before adding Hg^{2+}, Au@BSA/N6 was observed under dark field fluorescence microscopy with an excitation at 492 ± 18 nm and emission was collected using a triple pass emission filter, DAPI/FITC/TEXAS RED (DAPI, 452−472 nm; FITC, 515−545 nm; TEXAS RED, 600−652 nm), which showed red luminescence (Figure 2a−d). Details of the dark field microscopy setup are given in the Experimental Section of the Supporting Information.

These fibers were exposed to Hg^{2+} at various concentrations (1 ppb and 100, 50, and 20 ppt of Hg^{2+} solution); the quenching of red luminescence was observed as shown in Figure $2a_1$−d_1). The fibers were very sensitive to Hg^{2+}; the red color was quenched completely in 1 ppb, but even in the case of 20 ppt, a faint red color could be seen. The optical image of the fibers after the quenching experiments is shown in Figure $2a_2$−d_2. These images showed that there is no physical change in fiber dimension even after the quenching experiment.

The quenching experiments and fluorescence response of an ensemble of Au@BSA/FITC/N6 fibers on glass slides were conducted with various metal ions. Ions such as Mn^{2+}, Ni^{2+}, Cu^{2+}, Zn^{2+}, Pb^{2+}, and Cd^{2+}, chosen as they could be present in water with Hg^{2+}, did not induce any color change under florescence microscopy. Thus, the luminescence quenching is specific to Hg^{2+} as shown in Figure 3. About 5 μL of 20 ppm of

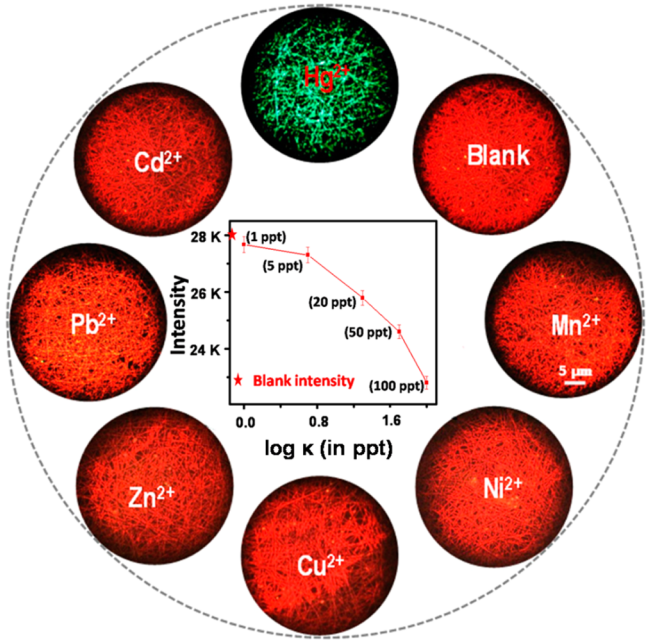

Figure 3. Images of sensing experiments using Au@BSA/FITC/N6 fiber mats with various metal ions. In the case of Hg^{2+} ion, the red luminescence of the cluster disappeared and a green color can be seen. For other metal ions, there is no change in red luminescence. It confirms that Au@BSA/FITC/N6 is selective to the Hg^{2+} ion. Inset: The variation of fluorescence intensity with different concentrations of the Hg^{2+} ion. It confirms that the limit of detection for mercuric ion is 1 ppt. The reduction in signal was more than three times the noise of the luminescence intensity of the parent fibers.

different metal ions was taken, and their quenching effect on Au@BSA/FITC/N6 fibers was investigated. It was first tested with water, and no quenching was observed. For other metal ions, quenching was not observed and the entire mat showed red luminescence. However, for Hg^{2+}, red luminescence quenched and green luminescence was visible due to FITC. Therefore, it confirms that Au@BSA/FITC/N6 is very sensitive and selective to Hg^{2+}. Emission spectra of mats under various conditions were measured. After measuring the spectrum of the Au@BSA/N6 fiber mats, the mats were dipped in different M^{2+} ion solutions (20 ppm). The mats were dried for 20 min, and then, the emission spectra of each mat was measured at 488 nm excitation. Variation in emission intensity is shown in Figure S3, Supporting Information. A large decrease in intensity was observed for Hg^{2+} compared to other M^{2+} ions. The sensing capability and limit of detection estimated from the luminecence spectra are shown in inset of Figure 3. Fluorescence spectra of Au@BSA/N6 fiber mats after exposure to varying concentrations of Hg^{2+} were measured. Fluorescence intensities of blank and Hg^{2+} treated fiber mats are compared in the inset of Figure 3. The experiment showed that the mats are sensitive even down to 1 ppt.

In Figure 4i, we examine the sensitivity limit at a single fiber level. A fixed volume (2.5 μL) of varying concentrations of Hg^{2+} (100, 20, and 10 ppt) was exposed to Au@BSA/FITC/N6 fibers separately. Red luminescence due to the cluster disappears, and the green luminescence due to FITC appears at 100 and 20 ppt Hg^{2+}. At 10 ppt, however, the decrease in red emission is barely observable. It did not quench completely, and as a result, a faint green luminescence is seen. An amount of 2.5 μL of 10 ppt Hg^{2+} translates to 7.5×10^7 ions. From

dx.doi.org/10.1021/ac502779r | Anal. Chem. 2014, 86, 10996−11001

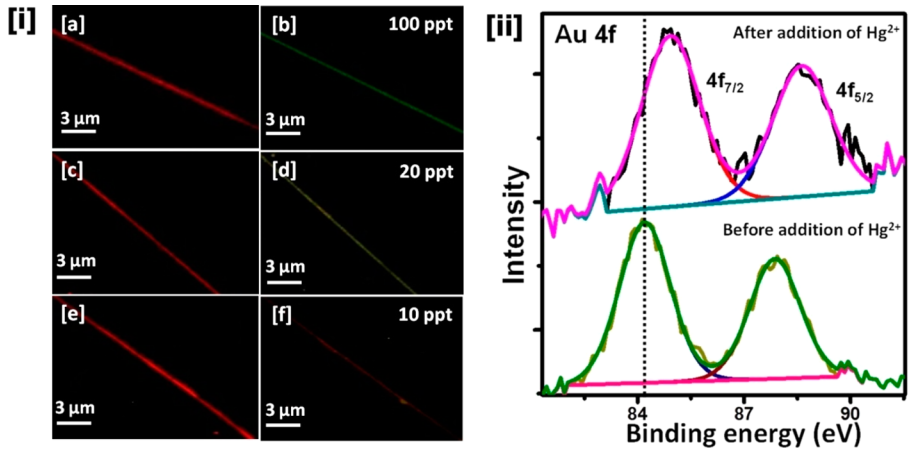

Figure 4. (i) (a, c, e) Fluorescence images of the Au@BSA/FITC/N6 single fiber showing red emission. Quenching experiment at (b) 100 ppt (green emission), (d) 20 ppt (green emission), and (f) 10 ppt Hg^{2+} (faint red emission). At 20 ppt, the fluorescence due to FITC is visible, and at 10 ppt, luminescence of Au@BSA is still observable. (ii) XPS spectra of the Au 4f region for the Au@BSA/N6 fiber mat before (down) and after (top) Hg^{2+} exposure. It shows that gold oxidizes due to the addition of the Hg^{2+} ion solution which may be responsible for the quenching of red luminescence of the Au@BSA cluster.

experiments conducted on glass substrates, we know that 2.5 μL of solution covers an area of 8.34×10^{-6} m^2 (details of calculation are given in Supporting Information, Section S4). The surface area of a 15 μm long fiber (typical length examined in an image) of 200 nm diameter is 9.41×10^{-12} m^2. The number of ions present in this area is ~80 which amounts to extremely low levels of detection. The level of sensitivity observed is extremely unusual. At this limiting concentration, the quenching is not complete, and therefore, the underlying green fluorescence does not appear distinctly, as mentioned earlier.

The response of a single fiber to the analyte is fast. As shown in the video (Supporting Information), the luminescence disappears as the Hg^{2+} solution wets the fiber from the top to the bottom. Response of the fiber is uniform as shown in Figure S5a, Supporting Information. Luminescence of one-half of Au@BSA/N6 fibers disappears as Hg^{2+} is exposed to the fibers (Figure S5b, Supporting Information). This is because the solution was exposed only to one-half of the fibers. The optical image of the fibers after Hg^{2+} addition shows that the fibers are intact (inset of Figure S5b, Supporting Information) although luminescence disappears. The data suggest that the fiber is uniformly exposed to the Hg^{2+} solution during wetting. We have observed the same changes for the Au@BSA/FITC/N6 fiber also (Figure S6, Supporting Information).

To demonstrate a real life application of our methodology, we have tested surface water from a well. We have added 2.5 μL of well water on a Au@BSA/N6 single fiber, and no quenching of luminescence was observed. We repeated the same experiment by adding 1 ppb of Hg^{2+} ions on the fibers. We have seen quenching of red luminescence of Au@BSA. It implies that the red luminescence of the fiber is selective to Hg^{2+} and not to other species in the natural water. The results are presented in Figure S7, Supporting Information.

To understand the reason behind the quenching of red luminescence on the addition of mercuric ion, we performed XPS analysis. XPS spectra in the Au 4f region of the Au@BSA/N6 fiber mat before and after addition of Hg^{2+} are shown in Figure 4ii. In the case of the cluster, Au is nearly in the zero oxidation state (with a binding energy (BE) of 84.1 eV for Au $4f_{7/2}$). The BE for Au is increased on treatment with mercuric ion (at 85.3 eV). Data suggest that mercuric ion (Hg^{2+}) oxidizes the Au core which is responsible for quenching of the red luminescence. Hg^{2+} uptake leads to Hg^0 implying its reduction on the fiber surface. The peak of Hg $4f_{7/2}$ is seen at 101.8 eV (Figure S8, Supporting Information).

CONCLUSION

In conclusion, we demonstrated a methodology for ultratrace Hg^{2+} detection using atomically precise clusters of gold coated on single nanofibers. The fibers present a highly sensitive, selective, and cost-effective way of sensing Hg^{2+} ions. The data show the possibility of sensing single ions at a single fiber level, when smaller lengths are examined. Electrospun nanofibers could be mass-produced at low-cost, allowing these novel sensing materials for field applications. Additional experiments are required to understand the reason for enhancement of emission of clusters on nanofibers.

ASSOCIATED CONTENT

Supporting Information

Figures S1−S8 and a video. This material is available free of charge via the Internet at http://pubs.acs.org.

AUTHOR INFORMATION

Corresponding Author

*E-mail: pradeep@iitm.ac.in.

Notes

The authors declare no competing financial interest.

ACKNOWLEDGMENTS

We thank the Department of Science and Technology, Government of India for constantly supporting our research program on nanomaterials. A.G. thanks the Council of Scientific and Industrial Research (CSIR) for a fellowship

REFERENCES

(1) Mathew, A.; Pradeep, T. *Part. Part. Syst. Charact.* **2014**, DOI: 10.1002/ppsc.201400033.

(2) Zheng, J.; Nicovich, P. R.; Dickson, R. M. *Annu. Rev. Phys. Chem.* **2007**, *58*, 409−431.

(3) Diez, I.; Ras, R. H. A. *Nanoscale* **2011**, *3*, 1963−1970.

(4) Jin, R. *Nanoscale* **2010**, *2*, 343−362.
(5) Choi, S.; Dickson, R. M.; Yu, J. *Chem. Soc. Rev.* **2012**, *41*, 1867−1891.
(6) Ghosh, S.; Anand, U.; Mukherjee, S. *Anal. Chem.* **2014**, *86*, 3188−3194.
(7) Cobley, C. M.; Chen, J.; Cho, E. C.; Wang, L. V.; Xia, Y. *Chem. Soc. Rev.* **2011**, *40*, 44−56.
(8) Liu, Y.; Ai, K.; Cheng, X.; Huo, L.; Lu, L. *Adv. Funct. Mater.* **2010**, *20*, 951−956.
(9) Lin, Y.-H.; Tseng, W.-L. *Anal. Chem.* **2010**, *82*, 9194−9200.
(10) Goswami, N.; Giri, A.; Bootharaju, M. S.; Xavier, P. L.; Pradeep, T.; Pal, S. K. *Anal. Chem.* **2011**, *83*, 9676−9680.
(11) Wang, X.; Wu, P.; Lv, Y.; Hou, X. *Microchem. J.* **2011**, *99*, 327−331.
(12) Wen, F.; Dong, Y.; Feng, L.; Wang, S.; Zhang, S.; Zhang, X. *Anal. Chem.* **2011**, *83*, 1193−1196.
(13) Retnakumari, A.; Jayasimhan, J.; Chandran, P.; Menon, D.; Nair, S.; Mony, U.; Koyakutty, M. *Nanotechnology* **2011**, *22*, 285102−285111.
(14) Mathew, A.; Sajanlal, P. R.; Pradeep, T. *Angew. Chem., Int. Ed.* **2012**, *51*, 9596−9600.
(15) Frenot, A.; Chronakis, I. S. *Curr. Opin. Colloid Interface Sci.* **2003**, *8*, 64−75.
(16) Zamani, M.; Prabhakaran, M. P.; Ramakrishna, S. *Int. J. Nanomed.* **2012**, *8*, 2997−3017.
(17) Kaur, S.; Sundarrajan, S.; Rana, D.; Sridhar, R.; Gopal, R.; Matsuura, T.; Ramakrishna, S. *J. Mater. Sci.* **2014**, *49*, 6143−6159.
(18) Jin, G.; Prabhakaran, M. P.; Ramakrishna, S. *Photochem. Photobiol.* **2014**, *90*, 673−681.
(19) Shin, M. K.; Kim, S. I.; Kim, S. J.; Kim, S.-K.; Lee, H.; Spinks, G. M. *Appl. Phys. Lett.* **2006**, *89*, 231921−231929.
(20) Shin, M. K.; Kim, Y. J.; Kim, S. I.; Kim, S.-K.; Lee, H.; Spinks, G. M.; Kim, S. J. *Sens. Actuators, B* **2008**, *134*, 122−126.
(21) Liao, Y.; Wang, R.; Fane, A. G. *Environ. Sci. Technol.* **2014**, *48*, 6335−6341.
(22) Gu, B. K.; Shin, M. K.; Sohn, K. W.; Kim, S. I.; Kim, S. J.; Kim, S.-K.; Lee, H.; Park, J. S. *Appl. Phys. Lett.* **2007**, *90*, 263901−263903.
(23) Diez, I.; Pusa, M.; Kulmala, S.; Jiang, H.; Walther, A.; Goldmann, A. S.; Mueller, A. H. E.; Ikkala, O.; Ras, R. H. A. *Angew. Chem., Int. Ed.* **2009**, *48*, 2122−2125.
(24) Ghosh, A.; Udayabhaskararao, T.; Pradeep, T. *J. Phys. Chem. Lett.* **2012**, *3*, 1997−2002.
(25) Xie, J.; Zheng, Y.; Ying, J. Y. *J. Am. Chem. Soc.* **2009**, *131*, 888−889.
(26) Shibu, E. S.; Pradeep, T. *Int. J. Nanosci.* **2009**, *8*, 223−226.
(27) Shibu, E. S.; Pradeep, T. *Chem. Mater.* **2011**, *23*, 989−999.
(28) Muhammed, M. A. H.; Shaw, A. K.; Pal, S. K.; Pradeep, T. *J. Phys. Chem. C* **2008**, *112*, 14324−14330.
(29) Habeeb Muhammed, M. A.; Pradeep, T. *Small* **2011**, *7*, 204−208.
(30) Reneker, D. H.; Yarin, A. L. *Polymer* **2008**, *49*, 2387−2425.
(31) Xia, Y.; Yang, P.; Sun, Y.; Wu, Y.; Mayers, B.; Gates, B.; Yin, Y.; Kim, F.; Yan, H. *Adv. Mater. (Weinheim, Ger.)* **2003**, *15*, 353−389.
(32) Kim, H. N.; Ren, W. X.; Kim, J. S.; Yoon, J. *Chem. Soc. Rev.* **2012**, *41*, 3210−3244.
(33) Nolan, M. A.; Kounaves, S. P. *Anal. Chem.* **1999**, *71*, 3567−3573.
(34) Du, Y.; Liu, R.; Liu, B.; Wang, S.; Han, M.-Y.; Zhang, Z. *Anal. Chem.* **2013**, *85*, 3160−3165.
(35) Sener, G.; Uzun, L.; Denizli, A. *Anal. Chem.* **2014**, *86*, 514−520.
(36) Xuan, F.; Luo, X.; Hsing, I. M. *Anal. Chem.* **2013**, *85*, 4586−4593.
(37) Xie, J.; Zheng, Y.; Ying, J. Y. *J. Am. Chem. Soc.* **2009**, *131*, 888−889.